

## The Gauribidanur radio observatory

Ch V Sastry

Indian Institute of Astrophysics, Bangalore 560 034

&

Raman Research Institute, Bangalore 560 080

The Raman Research Institute and the Indian Institute of Astrophysics in a joint collaboration program operate the Gauribidanur radio observatory. Details of the various antenna arrays and receiver systems available at the observatory are given. A brief account of the results obtained is also presented.

### 1 Introduction

The earth's atmosphere allows ground-based radio astronomical observations over a range of frequencies extending from a few megahertz to a hundred or more gigahertz. The high frequency limit exists because of absorption by water and oxygen in the atmosphere and the low frequency one because of refraction in the ionosphere. Observations made at frequencies of 30 MHz and below are generally referred to as low frequency, or decametric, measurements. This region of the radio spectrum is relatively un-explored owing to various reasons. Observations at low frequencies are difficult because of absorption, refraction and scintillation in the ionosphere. Among the other difficulties are the large antenna size necessary to achieve a reasonable resolution, and the very limited bandwidth which can be found free of man-made interference.

Decametric radio waves are emitted by a variety of astronomical sources which are much weaker or are not detectable at high frequencies. In this wavelength range, synchrotron radiations the dominant type from both galactic and extra-galactic sources, and synchrotron self-absorption becomes important. Information about magnetic fields and electron energy spectra in various types of sources can be derived from their decametric radio spectra. Free-Free absorption in the H-II region becomes significant at low frequencies, and its study can yield electron densities and temperatures in these ionized regions. Diffraction in both the interstellar and interplanetary media is very strong and can be used to study the medium itself or as a powerful tool in determining the size of small sources.

The Raman Research Institute and Indian Institute of Astrophysics in a joint collaboration program constructed a large decametre-wave antenna array and also a metre wave array at Gauribidanur (Lat: 13°36'12"N; Long: 77°26'07"). These tele-

scopes are being used for various types of astronomical investigations. Some characteristics of the telescopes and receivers are given. A brief account of the results obtained is also presented.

### 2 Telescopes

The main facility at the observatory is the decametre-wave radio telescope, operating at 34.5 MHz, which is essentially a meridian transit instrument although limited tracking capability is available. The telescope consists of 1,000 broadband dipoles arranged in the form of the letter T. A schematic of the dipole used in the array is shown in Fig. 1. The outputs of four such dipoles along the East-West direction are combined in a Christmas tree fashion using open wire transmission lines, transformers, and a balun to form a basic array element as shown in Fig. 2. Such basic elements, numbering 250 are arranged to form a 1.38 km long EW array along the East-West direction and a 0.45 km long S array extending southwards from the centre of the EW array as shown in Fig. 3.

The EW array consists of ten groups of 16 basic elements each. In each one of such groups, the 16 basic elements are arranged in the form of  $4 \times 4$  matrix. The outputs of the basic elements are combined as shown in Fig. 4 to produce a group output. Five group outputs, available from each of the East and West arms, are combined separately and the amplified outputs of the East and West arms are brought to the receiver room (Fig. 5).

The S array consists of 90 basic elements arranged along the N-S direction. The output of each element is amplified using a FET pre-amplifier. These amplified outputs are then combined together in a Christmas tree fashion using diode phase shifters, power combiners and amplifiers at appropriate stages as shown in Fig. 6. This final output is brought to the receiver room.

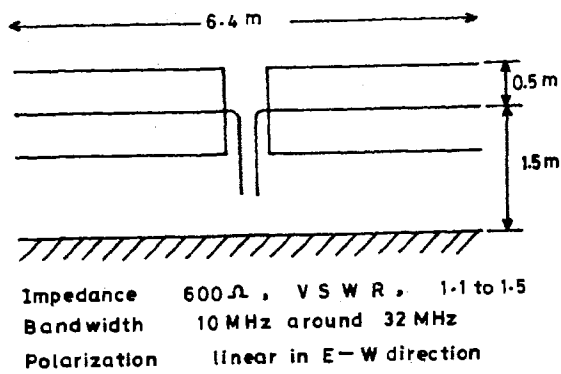


Fig. 1—A schematic of the dipole used in the T array

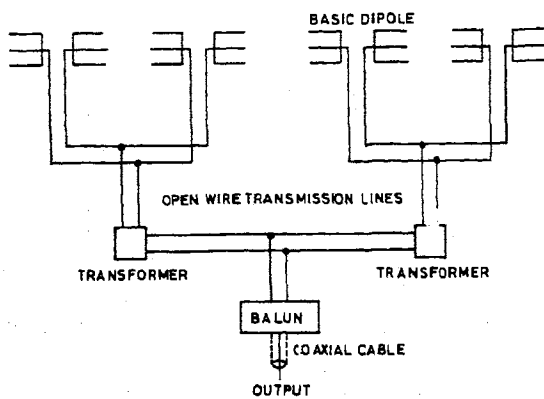


Fig. 2—A basic array element consisting of four dipoles connected in a branched feeder system

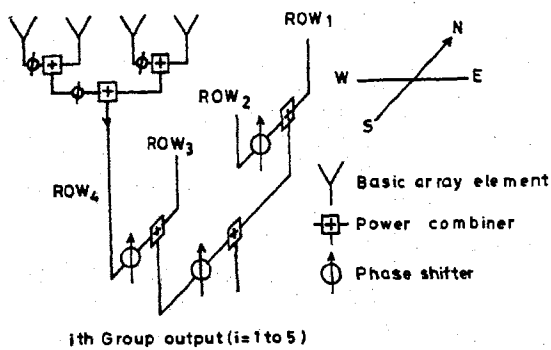


Fig. 4—Configuration within each East-West group

The beams of both the arrays can be tilted in the N-S direction by setting appropriate phase gradients along the N-S direction with the help of the diode phase shifters used in the feeder system. A special purpose control system is used to generate appropriate control signals for these phase shifters. When the outputs of the EW and S arms, are correlated in phase, a pencil beam of half power width  $26' \times 40'$  sec (z) arc is obtained, where z is the zenith angle. This correlation beam can be pointed to any direction along the meridian within a declination range of  $-45^\circ$  to  $+75^\circ$  in steps of  $12'$  arc. The time required

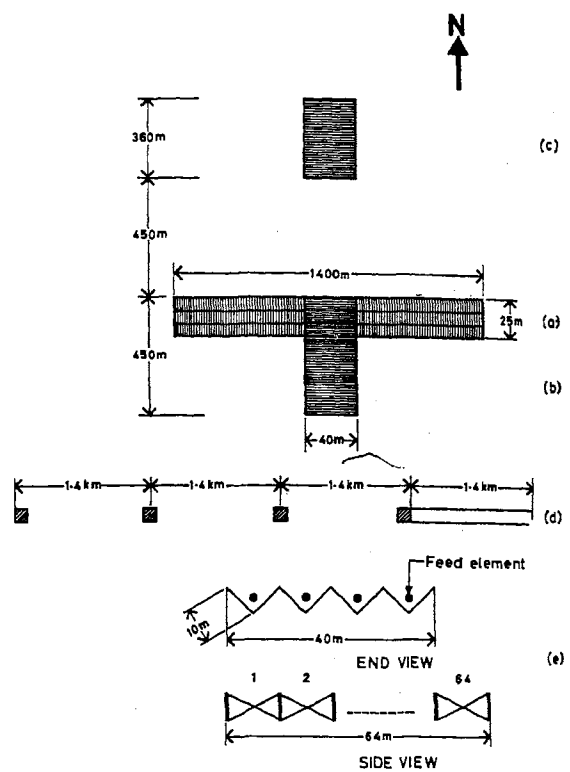


Fig. 3—Lay-out and dimensions of various antenna arrays at Gauribidanur (a) East-West array: 4 rows in N-S direction, 160 dipoles in each row; (b) South array: 90 rows in N-S direction, 4 dipoles in each row; (c) North array: 64 rows in N-S direction, 1 Yagi in each row; (d) Compound grating interferometer: E-W array and 4 grating units. Each grating unit consists of 8 Yagis; (e) Broadband array: 64 conical dipoles arranged in a matrix of  $4 \times 16$  along E-W and N-S directions respectively

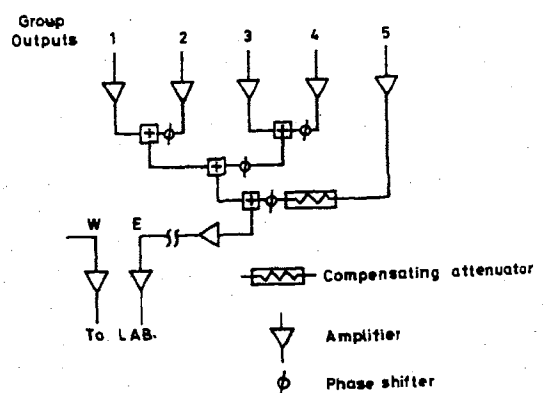


Fig. 5—Combination of groups in the East-West array

to change the beam from one position to another is about 10 ms and the number of declinations through which the beam is cycled can be varied from one to sixteen. The ideal beam patterns in the E-W and N-S directions, corresponding to the in-phase correlation, are close to sine functions. Because the beam-width in the E-W direction is  $26'$  arc, a point source

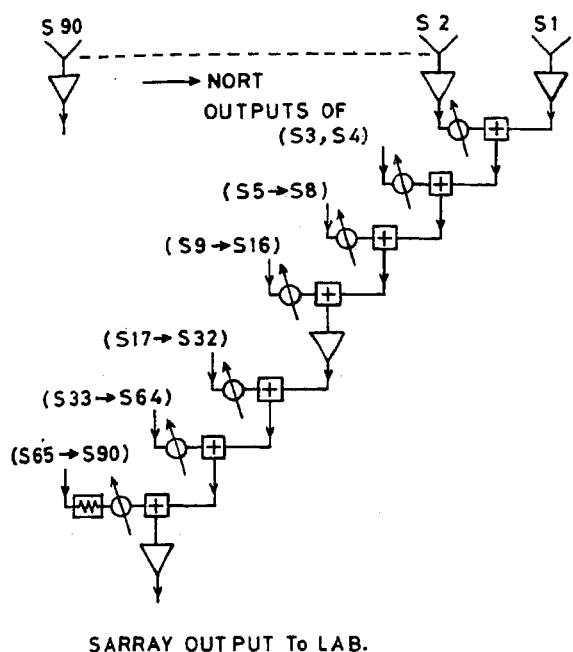


Fig. 6—Configuration of the South array

can be observed for only about 2 sec ( $\delta$ ) minutes in a day, where  $\delta$  is the declination of the source.

The point source sensitivity of this telescope, for continuum observations, is sufficiently high and confusion limited due to poor angular resolution. However, for observations of weak pulsar signals, low-frequency recombination lines and interplanetary scintillations, the sensitivity attainable with the meridian transit telescope is not adequate. A tracking system is incorporated in the E-W array to enable observations over longer periods with the maximum possible collecting area of the T array.

Using this system the E-W beam can be tilted in hour angle to  $\pm 7^\circ 5'$  from the meridian. This is achieved by introducing appropriate phase gradients across the E-W array using diode phase shifters. The control signals for the phase shifters are supplied by another special purpose digital control system. It is thus possible to observe a source for 42 sec ( $\delta$ ) minutes. Aerial photographs of the E-W and N-S arrays are shown in Fig. 7.

The effective area of the telescope is approximately 20,000 sq. metres at 34.5 MHz. The mean sky brightness at this frequency is about 10,000 K and so the minimum detectable flux density is of the order of 10 Jy ( $1 \text{ Jy} = 10^{-26} \text{ watts}^{-2} \text{ Hz}^{-1}$ ) with an integration time of 24 s and a bandwidth of 400 kHz. The minimum detectable brightness temperature variations are of the order of 1000 K.

As pointed out above, the presence of many unresolved sources in the main beam results in a confu-



Fig. 7(a)—Aerial view of the East-West array from the eastern end

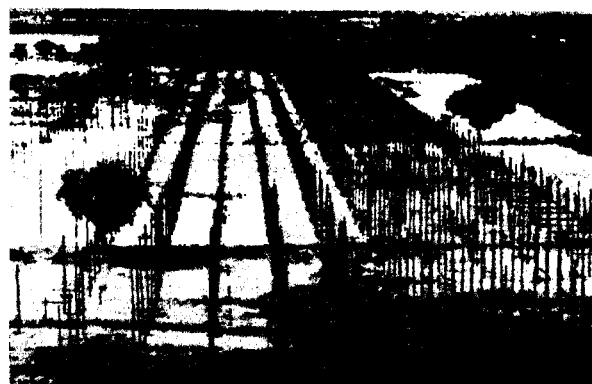


Fig. 7(b)—Aerial view of the South array from South-end

sion limit of the order of 10 Jy for the T array. It is therefore not possible to decrease the minimum detectable flux limit by increasing the integration time. In order to increase both the resolving power and the sensitivity, an array of 64 Yagis has been added to the T. This array is located at a distance of 0.45 km from the centre of the E-W arm of the T as shown in Fig. 3. The beam of this array can be pointed anywhere within  $\pm 50^\circ$  of the zenith on the meridian using diode phase shifters and a digital control system. The sum of the outputs of the north and south arrays can be multiplied with the E-W array to produce a beam of 26 arc min  $\times$  20 arc min at the zenith. A photograph of the north array is shown in Fig. 8.

High resolution one-dimensional observations are made with a compound grating interferometer with an E-W fan beam of three arc min. It consists of four grating units placed at intervals of 1.4 km (length of the E-W array) on an E-W base line starting from the western end of the E-W array as shown in Fig. 3. Each grating unit comprises of 8 Yagi antennas and the outputs of each one of them is multiplied with the EW array output to synthesize the fan beam.

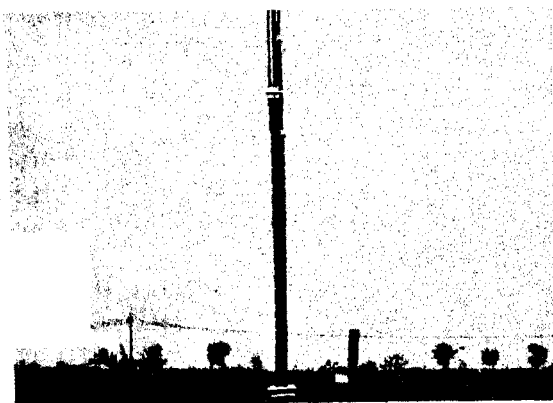


Fig. 8—North array of 64 Yagis

We also have a broadband array usable in the frequency range 30 to 70 MHz mainly for solar observations, a photograph of which is shown in Fig. 9. The basic element of this array is a biconical dipole with a VSWR  $\leq 2$  in the above frequency range. The array consists of 64 elements arranged in a matrix of  $4 \times 16$  along E-W and N-S directions respectively. The dipoles are placed inside a corner reflector and accept N-S polarization. The array is split up into northern and southern groups of eight rows each. The eight rows of each group are combined in a branched feeder system and delay shifters are introduced at appropriate places, to steer the response of the array to  $\pm 45^\circ$  of the zenith in the N-S direction. The position of the beam formed is independent of frequency allowing simultaneous observation of a radio source over the full bandwidth of the system. This array is also used in transit mode and the available observing times range from 26 minutes at 65 MHz to about an hour at 35 MHz. The effective collecting area is about 2000 m<sup>2</sup> and the sensitivity is better than 100 Jy at 65 MHz for a bandwidth of 1 MHz and 1 s integration time.

### 3 Receivers

The receiving systems available include several analog receivers and a 128 channel digital correlation receiver. The bandwidths and time-constants of the analog receivers are selectable in the range 15 to 1000 kHz and 10 ms to 30 s, respectively. The digital receiver is a double sideband system with one bit correlators. This receiver can also be configured as an autocorrelation spectrometer for spectral line and pulsar observations. A microprocessor based data acquisition and recording system is used for recording both analog and digital data. The system can accept 64 single ended channels at a maximum rate of 25 ms per channel. An acousto-optic spectrograph (AOS) provides high time and frequency

resolution for studies of radio bursts from the sun. The AOS has a bandwidth of 30 MHz with 1760 channels, with a frequency resolution of about 30 kHz. The spectrograph is interfaced via an A/D converter and a memory bank to VAX 11/730 computer. All its 1760 channels are scanned every 250 ms and the data are recorded either on the user disk of the computer or magnetic tape units.

### 4 Computer System

The VAX 11/730 system is available for off-line processing and data acquisition with the AOS system. It is supported by a 32 bit high speed microprogrammed central processing unit, 1 Mb RAM memory, 4 K ROM memory for control programs and two cartridge tape drives. Two drives of 20 Mb virtual memory and a tape drive which records at densities of 800/1600 bytes per inch are also available.

### 5 Observations and Results

The telescope is used for observations of the sun, galactic sources, background survey, and also extragalactic sources. Some of the important results of these observations are presented below.

#### 5.1 Sun

We have used the radio telescope to produce radio maps of the continuum emission from the quiet sun and active regions at decametric wavelengths. These are the first maps of this kind produced anywhere in the world. These maps were used to derive the temperature and density structure of the outer corona. Typical maps obtained during the sunspot minimum year 1983 are shown in Fig. 10. One-dimensional scans of the sun with a resolution of three arc minute are also made and used to study some properties of coronal holes. The acousto-optic spectrometer along with the broadband antenna array is used to study solar radio bursts with very high resolution in time and frequency as illustrated in Fig. 11.



Fig. 9—Broadband array of 64 biconical dipoles

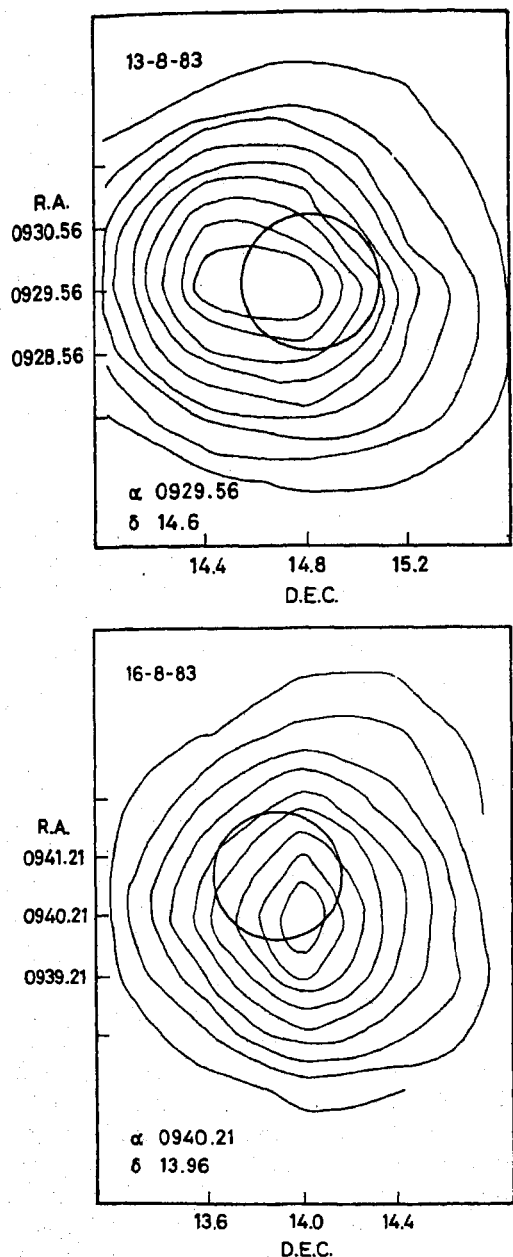


Fig. 10—Two radio maps of sun at 34.5 MHz obtained with the T array during August 1983. The optical disk of the sun is shown as a full circle.

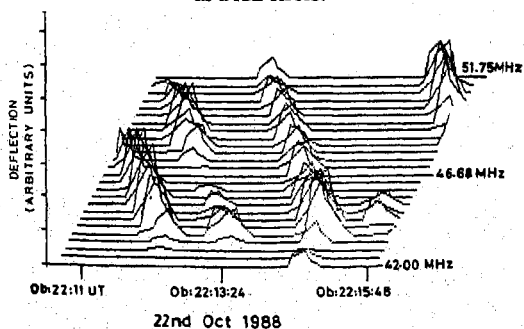


Fig. 11—Profiles of solar radio bursts obtained with the acousto-optic spectrograph between 42.00 and 51.75 MHz

5.2 Galactic Sources

*Supernova remnants*—The telescope has been used to study the structure of extended supernova remnants at decametre wavelengths. Radio maps of some of these remnants were made and the map of the Cygnus Loop is shown in Fig. 12. We were able to determine the variation of the low frequency spectral indices across these remnants and also test some of the theoretical models for the generation of radio emission in supernova remnants. The reduction in the low frequency flux density in some cases is shown to be due to absorption in the interstellar medium.

5.3 Ionised Hydrogen Regions

The decametrewave radio telescope is the most sensitive detector of ionised hydrogen regions (H-II) in the galaxy. The temperature of these regions is usually  $\leq 10,000$  K and so they appear as continuum absorption features against the very bright non-thermal background radio emission from the galaxy. It is possible to measure the electron temperature of H-II regions directly unlike in high frequency measurements where one has to assume LTE conditions in the nebulae to derive the temperatures. We have mapped the H-II regions Rosette Nebula and the giant complex known as W51 in continuum absorption, and determined the mean electron kinetic temperatures. We were also able to show that the H-II region in the complex W51 is surrounded by a non-thermal ring which is probably a supernova remnant.

5.4 Pulsars

Pulsar observations with the T array were initially made with a single frequency analog correlation re-

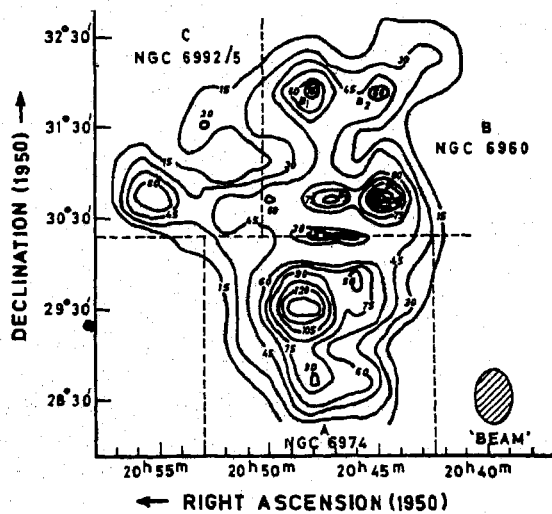


Fig. 12—Radio map of the supernova remnant, Cygnus Loop, at 34.5 MHz made with the T array

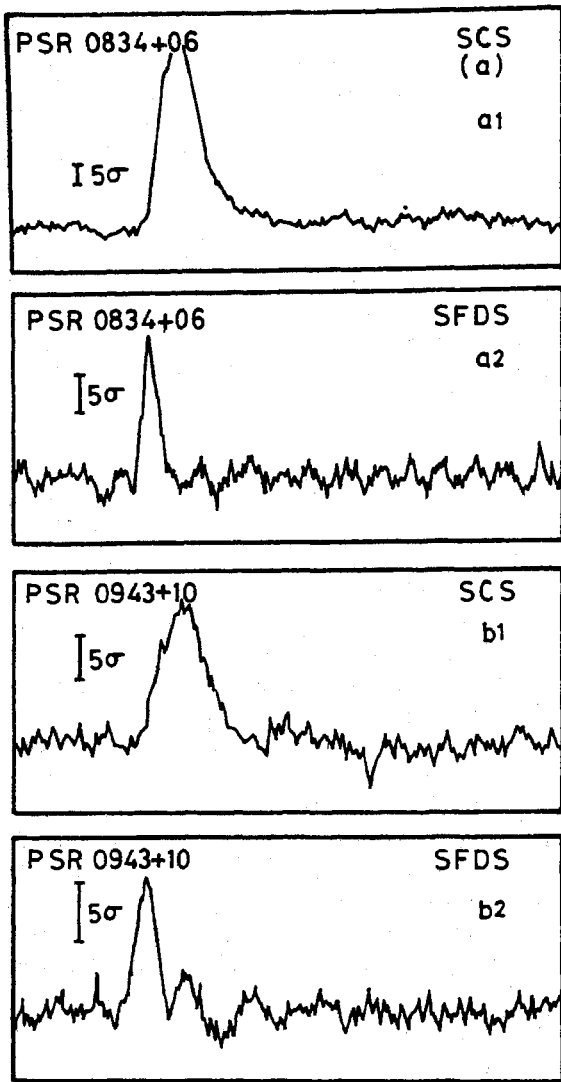


Fig. 13—Average pulsar profiles SCS, single channel scheme; SFDS, swept frequency dedispersion scheme. (a<sub>1</sub>, a<sub>2</sub>) 0834 + 06 effective integration: 24 minutes ( $p=1.2737645S$  and  $DM=12.855\text{ cm}^{-3}\text{ pc}$ ). (b<sub>1</sub>, b<sub>2</sub>) 0943 + 10 effective integration: 72 minutes ( $p=1.0977045S$  and  $DM=15.35\text{ cm}^{-3}\text{ pc}$ )

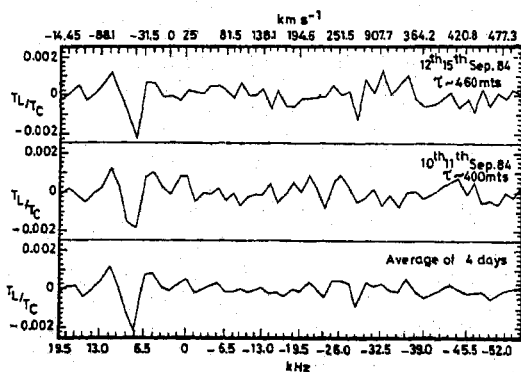


Fig. 14—Observed profiles of low frequency recombination lines C574 and C575 and 34.5 MHz in the direction of Cas A

ceiver using the tracking facility which allows observations for  $42 \times \text{sec}$  (Declination) minutes. The data processing consists of folding over a two period stretch and testing for significant detection of two similar pulses separated by one period. To improve the (S/N) ratio, data from different days were averaged. Subsequently a digital autocorrelation receiver and a swept frequency local oscillator system were used. The local oscillator was swept over the bandwidth of the receiver at a rate determined by the dispersion measure of a given pulsar and the autocorrelation function (ACF) was measured. The pulse profiles were obtained from the ACF by further processing. The time profiles of the pulses from two pulsars obtained using both the techniques are presented in Fig. 13. The important results of our pulsar observations are high resolution pulse profiles and accurate estimates of pulse energies for eight pulsars. We have also found that the interpulse emission is absent at this frequency in many cases and that the intrinsic pulse widths do not follow any fixed scaling law with frequency.

### 5.5 Recombination Lines

The 128-channel digital correlator was used in the autocorrelation spectrometer mode along with the south array to search for recombination lines in absorption in the direction of strong radio sources. The C574 $\alpha$  and C575 $\alpha$  lines were detected in the direction of Cassiopeia A and are shown in Fig. 14.

### 5.6 Background Survey

The 128-channel digital correlation receiver was used for the survey of the entire accessible sky from Gauribidanur. For this purpose, the south array was divided into 23 groups and the output of each group was correlated with the E-W arm output to measure the complex visibilities. The brightness distribution is obtained by Fourier transforming the visibility data. A preliminary map of the galactic centre region is presented in Fig. 15 and all the sky maps will be published elsewhere.

### 5.7 Extra-galactic Sources

One of the most interesting observations made with the decametre radio telescope in the study of extra-galactic sources was the mapping of the diffuse radio emission from the Coma cluster of galaxies. The observation of intergalactic matter is of great importance in astrophysics, since it provides the gravitational forces necessary to bind together clusters of galaxies and indeed the entire universe. The observed radio luminosity of the diffuse source is  $10^{41}\text{ ergs}^{-1}$ . The magnetic field in the intergalactic

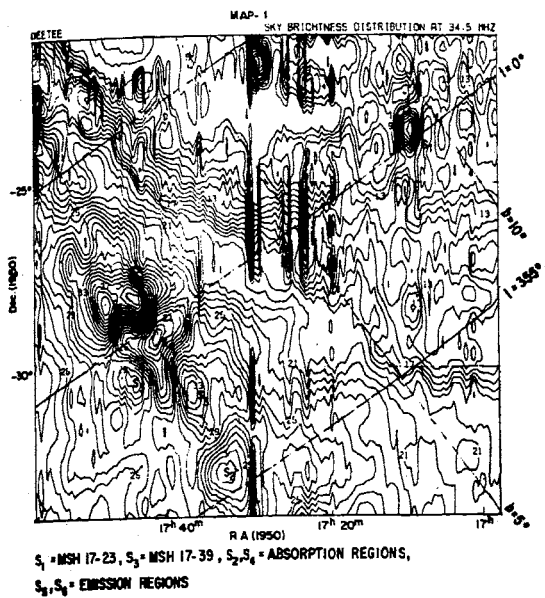


Fig. 15—Radio map of the galactic centre region at 34.5 MHz made with the T array

medium of the Coma cluster can be estimated by assuming the minimum energy condition in which the magnetic energy density is equal to the particle energy density and is approximately equal to two microgauss. This indicated that relativistic electrons must have been ejected from the radio galaxies in the cluster at a mean rate of  $10^{51}$  erg Yr<sup>-1</sup> for the past 3.5 billion years.

#### Acknowledgement

The author thanks Prof. V Radhakrishnan for his kind support and advice in all phases of this work. R K Shevgaonkar, K S Dwarakanath, A A Deshpande, K R Subramanian, N Uday Shankar and P S Ramkumar have contributed significantly to the various aspects of the work reported here. G N Rajasekhara, C Nanje Gowda, S Aswathappa and A T A Hameed assisted in the construction, maintenance and observations.